STRUCTURAL MRI
AND BRAIN DEVELOPMENT

[1]Paul M. Thompson PhD, [1]Elizabeth R. Sowell PhD, [2]Nitin Gogtay MD,
[2]Jay N. Giedd MD, [1]Christine N. Vidal, [1]Kiralee M. Hayashi,
[1]Alex Leow MD PhD, [3]Rob Nicolson MD,
[2]Judith L. Rapoport MD, [1]Arthur W. Toga PhD

[1]Laboratory of Neuro Imaging, Brain Mapping Division, Dept. of Neurology,
UCLA School of Medicine, Los Angeles, CA
[2]Child Psychiatry Branch, NIMH, Bethesda, MD

Book Chapter for *International Review of Neurobiology*
Guest Editor: Michael Glabus, Ph.D.
Submitted: January 17, 2005

Please address correspondence to:
Dr. Paul Thompson
(Room 4238, Reed Neurological Research Center)
Laboratory of Neuro Imaging, Dept. of Neurology,
UCLA School of Medicine
710 Westwood Plaza, Los Angeles, CA 90095-1769, USA
Phone: (310) 206-2101 **Fax:** (310) 206-5518 **E-mail:** thompson@loni.ucla.edu

Acknowledgments: This work was funded by grants from the National Institute for Biomedical Imaging and Bioengineering, the National Center for Research Resources, and the National Institute on Aging (to P.T.: R21 EB01651, R21 RR019771, P50 AG016570), by the National Institute of Mental Health, the National Institute of Drug Abuse, and the March of Dimes, (to E.R.S.: K01 MH01733, R21 DA15878, R01 DA017831, MOD 5FY03-12), and by the following grants from NCRR, NIBIB, NINDS and NIMH: PO1 EB001955, U54 RR021813, MO1 RR000865, and P41 RR13642 (to A.W.T.). Additional support was provided by NIMH intramural funding (N.G., J.N.G., J.L.R.).

Abstract

MRI scans provide exceptionally detailed information on how the human brain changes throughout childhood, adolescence, and into old age. We describe several approaches for understanding developmental changes in brain structures based on MRI. Atlas-based "parcellation" methods, for example, measure volumes of brain substructures, revealing how they change with age. Growth curves for different brain structures can be compiled, describing the expected trajectories of normal development. Additional computational anatomy techniques can be used to map spatial patterns of brain growth and tissue loss in individual children. Changes in cortical features, such as gray matter thickness, asymmetry, and complexity, can also be mapped. Individual maps can then be combined across subjects to make statistical maps or dynamic "time-lapse movies" that reveal systematic features of brain development in population subgroups, while retaining information on their variance. We review several large-scale studies of brain development, including longitudinal studies in which children were scanned repeatedly with structural MRI at 2-year intervals for periods of up to ten years. Image processing algorithms were then applied to recover detailed information from the resulting image databases. We describe the approaches necessary to compare brain MRI data across groups differing in age, covaried with gender, developmental disorders, or genotype. These methods reveal unsuspected links between development and cognition, and can help discover genetic and environmental factors that affect development. These brain maps also chart the anatomical sequence of healthy brain maturation and visualize how it is derailed in neuropsychiatric disorders such as schizophrenia, autism, fetal alcohol syndrome, and Williams syndrome.

1. Introduction

The quest to understand how the human brain develops is one of the most fascinating challenges in modern science. Brain cells proliferate in early embryonic life, in a carefully orchestrated sequence of neural cell migration and maturation. This leads to a human brain with around 100 billion neurons at birth. A newborn child's brain is only a fifth of its adult volume, and it continues to grow and specialize according to a precise genetic program, with modifications driven by environmental influences, both positive and negative. Negative environmental influences, such as malnutrition, maternal drug abuse, or viral infection, can impair or delay brain development. With stimulation and experience, the dendritic branching of neurons greatly increases, as do the numbers of synaptic connections. As layers of insulating lipids are laid down on axons through the process of myelination, the conduction speed of fibers that interconnect different brain regions also increases a hundredfold. This exuberant increase in brain connections is followed by an enigmatic process of dendritic 'pruning' and synapse elimination, which is thought to lead to a more efficient set of connections that are continuously remodeled throughout life.

MRI scanning of the brain can document these large-scale processes of brain development in detail. It enables insight into the sequence and timing of these developmental processes, documenting how they occur in living subjects. Individual brain scans provide exquisitely detailed maps of the brain's anatomy, while functional and metabolic scans (e.g. functional MRI and PET scans) provide complementary information on brain activation and physiology, as these change and mature.

In the 1990s, databases began to be assembled containing brain scans from hundreds of children scanned repeatedly over time (Jernigan et al., 1991; Reiss et al., 1996; Gogtay et al., 2004; Giedd et al., 2005). Repeated scanning of the same individual at different times during brain development makes it possible to capture "snapshots" of these growth processes, and reconstruct dynamic maps that describe how they play out in time. This wealth of anatomical data has in turn fueled the development of sophisticated image processing techniques that measure growth rates for different brain structures (Lange et al., 1997; Giedd et al., 1999; Thompson et al., 2000). These developmental patterns vary during adolescence and over the adult lifespan (Sowell et al., 1999, 2003, 2004), and they differ in clinical populations with developmental disorders (Rapoport et al., 1999; Gogtay

et al., 2005). More recently, time-lapse movies have been reconstructed to describe the dynamic sequence of cortical development (Gogtay et al., 2004, 2005). They show shifting patterns of tissue growth and loss, even in healthy children. These processes are thought to be exaggerated or derailed in those with early-onset schizophrenia and bipolar illness (Thompson et al., 2001, 2003; Gogtay et al., 2004). Finally statistics have been developed to capture how growth rates differ among brain substructures. With this normative data in hand, brain deficits in a variety of developmental disorders can be more readily distinguished from changes within the normal range.

At the cutting edge of these neuroimaging projects are worldwide efforts to identify factors that affect brain development positively or negatively. Quantitative *genetic* maps of the brain can clarify how genes and environmental factors (such as family upbringing, skill acquisition and learning) and impact development, as well as cognition and intelligence (Thompson et al., 2001; Gray and Thompson et al., 2004; Cannon et al., 2005). Other brain mapping efforts are discovering how neurological or psychiatric disorders affect the brain and how, and where in the brain, medications prevent or retard these changes. As such, MRI data is a witness to the sequence of brain development. Some of the observed changes correlate strongly with clinical, behavioral and cognitive differences, but in other cases, the cellular basis for the changes is not yet completely understood (Bartzokis et al., 2004).

In this chapter, we review imaging advances that have revealed new information on brain development. Although the imaging technologies themselves are maturing (e.g. functional MRI and diffusion imaging of fiber pathways), a quiet revolution is occurring in the analysis techniques to obtain information from the resulting brain images. In some respects, progress in the image analysis arena has vastly improved the power of MRI. Here we focus on the new information that these image analysis techniques offer, what they have revealed about normal brain development, and what they have found in a variety of childhood brain disorders (e.g., early-onset schizophrenia, autism, fetal alcohol syndrome, and genetic disorders such as Williams syndrome).

We first summarize some basic information on brain MRI and the structural development of the brain. We then analyze these changes in more detail with brain maps and time-lapse movies.

2. MRI Scanning and Image Analysis

3D Anatomical Scanning By the early 1990s, MRI was gradually replacing CT (computed tomography, or CAT scanning) as the technique of choice to image brain structure. Based on nuclear magnetic resonance (Bloch, 1946, Lauterbur, 1973), MRI scanning requires no ionizing radiation (i.e., no radioactive tracers or exposure to X-rays), so it is safe for use in developmental studies of children, and for repeated image acquisitions over time. A detailed description of MRI physics is provided elsewhere (Elster, 1994). Briefly, the subject is placed in a strong magnetic field created by a superconducting magnet surrounding the bore of a scanner. The subject, lying in the scanner, is exposed to brief pulses of radio-frequency radiation from a transmission coil around the subject's head. The energy of a radio-frequency signal transmitted into the brain tissue can be absorbed by the nuclei of its constituent hydrogen atoms. This energy is then released, and the rate at which it is released (magnetic 'relaxation') depends on the local molecular environment (differing, for example, in gray and white matter). Gray and white matter, as well as other tissues, can therefore be distinguished with MRI.

MRI scanners are also programmed to create spatial gradients in the underlying magnetic field. The spatial location of tissues with different molecular content is retained using Fourier encoding, creating an MR image. A typical MR image is shown in Fig. 1(a). Note the clear intensity contrast between gray matter structures (such as the cortex and basal ganglia) and the intervening white matter (consisting of myelinated fiber pathways that interconnect brain structures). The quantity of gray and white matter in the brain, as well as cerebro-spinal fluid (CSF) in the ventricles and cortical sulci, can therefore be computed and compared across subjects and over time. To create maps of tissue types (Fig. 1(b)), tissue classification (or "segmentation") algorithms can be used. These

computer programs typically model the intensities in the image as arising from a set of Gaussian functions. By estimating the parameters of these functions, the programs infer how likely it is that each pixel in the image is primarily made up of gray matter, white matter, CSF, or a background class (e.g. consisting of dura and meningeal tissue, or air surrounding the head). Once the 3D maps of these tissue classes are determined, their volumes are measured. They may also be subdivided into smaller regions to determine the amount of each tissue type in each lobe (see e.g. Fig. 1(c)).

Types of MRI Analysis. Regional volumes of brain structures can be analyzed statistically. Most commonly, total brain volumes and regional volumes are computed for gray and white matter in specific lobes of the brain, as well as volumes for deep gray matter nuclei, such as the basal ganglia and hippocampus (Jernigan et al., 1991; Kennedy et al., 1998). MRI analysis methods have advanced significantly in recent years. We discuss three such methods (with increasing complexity) that have each yielded considerable information about brain development. These are:

1. Parcellation methods. In these, an image analyst uses a formalized anatomical protocol (usually based on a brain atlas or rules agreed on by anatomists) to trace the boundaries of individual structures in cross-sections from each MRI scan. In a more automated version of this approach, a standard anatomical brain dataset, such as a digital brain atlas, is labeled by hand, and is elastically deformed or 'warped' onto the MRI datasets, adapting to variations in individual anatomy (Collins et al., 1995; see Thompson and Toga, 2003 for a review of these "deformable atlas" approaches). By transferring the labels from the digital atlas to the MRI scan of the individual aligned with it, 3D models of the structure in each individual are then reconstructed. Depending on how well the atlas anatomy fits that of the individual, this process may be automated, or the structure models may be treated as approximate and adjusted later by hand. The measured volumes can then be analyzed statistically, e.g. with multiple regression or analysis of variance, to assess the magnitude and significance of any changes with age (Fig. 2), or gender differences. Group differences in brain structure can also be assessed, and factors can be identified that correlate with regional brain volumes, such as gender (Fig. 3), genotype, or disease, or clinical measures obtained from the subjects in the study. See Chapter 1 (*this volume*) for a more detailed description.

2. Anatomical Mapping Methods. Rather than splitting the brain up into components, these methods provide 3D statistical *maps* of anatomy for different groups of subjects, or subjects of different ages. Group average maps of anatomy can be computed and compared, to identify where differences in brain structure can be detected. Maps of statistics are compiled showing brain regions with statistical differences in structure across groups. Regions can also be identified that show significant changes in specific tissue parameters (e.g. gray matter thickness, hemispheric asymmetry) over time. Before brain maps can be created, multiple brain MRI datasets are first aligned into a common 3D coordinate space, so that anatomy can be indexed using 3D coordinates. Geometrical models of structures are then reconstructed for each individual, often by hand, or with the aid of automated software. These models are sometimes represented as geometrical surfaces in 3D, and their shape can be averaged across subjects to provide a composite or 'average' representation of anatomy for a group. Quantitative maps and models can then be made to show shape changes, as well as growth and atrophy in specific structures such as the hippocampus (Csernansky et al., 1999; Narr et al., 2000; Thompson et al., 2004), corpus callosum (Sowell et al., 2001a), or basal ganglia (Thompson et al., 2000). The cortical surface provides unique challenges when trying to find consistent and systematic patterns of change during development. Because gyral patterns of the cortex differ markedly across individuals, more complex methods are required to average and compare cortical data across subjects and groups. One such approach is called *cortical pattern matching*, which we describe below (Fig. 4; Thompson et al., 2004).

3. Time-Lapse Movies. Anatomical modeling methods can be used to create static statistical maps of anatomy, and the same idea can be extended to create dynamic representations, illustrated as *time-lapse movies.* These animations reveal how specific features of the brain (e.g. gray matter thickness, or cortical shape) change with age, over the entire human lifespan, or in specific diseases. So far these movies have been used to track shifting

processes of cortical development in childhood and adolescence (Gogtay et al., 2004), subtle changes with normal aging (Sowell et al., 2003), and progressive brain deficits in schizophrenia (Thompson et al., 2001) and Alzheimer's disease (Thompson et al., 2003). Time-lapse movies can be made for any brain structure (Thompson et al., 2004 for an example mapping the hippocampus and ventricles). Cortical time-lapse movies can be made by combining cortical pattern matching methods with statistical models that describe how different attributes of the cortex change over time.

3. Growth Curves for Different Brain Regions.

To illustrate the application of these methods, we describe data from an ongoing longitudinal pediatric brain MRI study at the Child Psychiatry Branch of the National Institute of Mental Health. To date over 1000 scans have been analyzed, and Fig. 2 shows data on total brain volume from 224 girls and 287 boys. These children are evaluated with MRI and neurocognitive testing at approximately 2-year intervals, and the images are analyzed with a combination of manual and automated tracing techniques in collaboration with imaging centers throughout the world. Data on regional brain volumes were obtained in collaboration with the Montreal Neurological Institute, and brain maps and movies were created in collaboration with the UCLA School of Medicine.

Fig. 2 shows that brain volume is about 90% of its final adult volume by age 6, and girls' brains are on average around 12% smaller than boys'. This gender difference is explained largely by differences in height and is not thought, in itself, to account for any gender differences in cognitive domains (see Kimura, 1999, for a review of these differences). Despite this overall gender difference in brain volume, it is worth noting that it would be hard to distinguish the brain MRI scan of a boy or a girl on the basis of brain volume or any other MRI parameter given the large inter-subject variability as illustrated in Fig. 2.

Gray Matter in Each Lobe of the Brain. The earliest pediatric brain MRI studies suggested that gray matter (GM) volumes generally declined after age 5, perhaps because the advancement of white matter myelination throughout childhood began to overtake the overall rate of brain volume expansion, causing a net decrement in the amount of tissue appearing gray (or unmyelinated) on MRI. The distinction of gray and white matter in the neonate brain is somewhat artificial as axonal fiber tracts are not sufficiently myelinated at birth to appear brighter (i.e. hyperintense) on T1-weighted MRI. Later longitudinal studies found that cortical gray matter volume increased throughout childhood, peaking in early or late adolescence, and falling thereafter. Giedd et al. (1999) compiled normative growth curves for each of the lobes of the brain, demonstrating the hetrochronous nature of brain development, in which the different lobes develop at different rates. Parietal, frontal and temporal GM volumes peaked at ages 11.8, 12.1, 16.2 in boys, and at ages 10.2, 11.0, 16.7 years in girls.

Modeling Developmental Trajectories with Mixed Models. The trajectories plotted in Figure 2 are computed using *mixed models*, or random effects models, a statistical technique that allows both longitudinal and cross-sectional data to be combined to compute a single average trajectory of development for a specific brain measure. It is worth describing how these curves are actually computed. For the *i*th individual's *j*th measure we have:

$$Y_{ij} = f(\mathrm{Age}_{ij}, \underline{\beta}) + \varepsilon_{ij} \qquad (1)$$

Here Y_{ij} is the outcome measure derived from the brain scan, such as a tissue volume for a particular lobe, $f()$ is a constant, linear, quadratic, cubic, or other function of the individual's age for that scan and the regression/ANOVA coefficients to be estimated are included in a vector, $\underline{\beta}$. In studies with multiple scans over time, it is usual to fit a random effects model with correlated errors:

$$Y_{ij} = \alpha_i + f(\mathrm{Age}_{ij}, \underline{\beta}) + \varepsilon_{ij} \qquad (2)$$

Here the model is the same as the General Linear Model except for the α_i term, which is called a random effect (Davidian and Giltinan, 1995; Verbeke and Molenberghs, 1997). ε_{ij} and ε_{ik} (k not equal to j) are assumed correlated, and the correlation is a function of the time that has elapsed between the two measurements. In our own work, we typically use the SAS nonlinear 'PROC MIXED' function to develop equations that model each brain variable as a quadratic function of age, incorporating random person effects for the intercept terms, and employing SAS MIXED's capacity to model spatial covariance between the repeated measures as a function of the time span between the two measurements for each participant (Thompson et al., 2004). We usually implement the simpler models directly in C and validate them against SAS. Our general strategy is to model growth curves using mixed model analyses including covariates and interaction terms to test hypothesized differences among various strata (e.g. gender differences or disease effects; Gogtay et al., 2005).

Trajectories in Large Samples of Subjects. Fig. 3 shows the plots obtained by fitting a cubic model to age-related changes in total cerebral volume, total gray and white matter, frontal gray matter, and the volume of a particular substructure, the cerebellum (data from Giedd et al., 2005). In this largest MRI study of brain development to date (224 females, 287 males), the total volume of the brain rose gently until puberty in boys and girls (with a higher and later peak in boys), and then followed a very gradual decline. When these changes are split into white matter and gray matter components, the white matter volume continued to increase rapidly throughout the teenage years, increasing both in absolute terms, and as a proportion of brain volume, well after puberty and into adulthood. In Sowell et al., 2003, we were able to fit a quadratic model to whole brain white matter volumes over the lifespan. This cross-sectional study evaluated 176 healthy subjects between the ages of 7 and 87. In agreement with earlier reports by Bartzokis et al. (2003) and others, the white matter volume appeared to peak in the mid-forties, and its overall trajectory was well-described by a quadratic (inverted 'U') profile, despite considerable individual variation.

Mechanisms. It is tempting to try to break down these changes into several hypothetical processes that might lead to gray and white matter gain and reduction, and relate them to those that are known to occur on a cellular level. The white matter volume expansion is not attributed to the emergence of additional axonal fibers. Instead myelination increases the volume of the insulating sheaths surrounding axonal fibers and bulks up the volume of the white matter compartment. This process can also be seen as increased white matter diffusion anisotropy with diffusion tensor imaging (DTI), as greater myelin deposition increasingly constrains the diffusion of water within axons. By mid-life (40's), white matter breakdown overtakes the process of increased myelination and the net effect is a white matter volume decline. Age-related myelin breakdown can be readily visualized with electron microscopy. It consists primarily of splits in the lamellae of the myelin sheaths or ballooned sheaths in the absence of neuronal or synaptic loss (Peters et al. 2000; Nielsen and Peters, 2000). This myelin degeneration creates microscopic fluid filled spaces, and increases in MR-detectable water, and thus decreases in the relaxometric parameter, R_2 (Englund et al. 1987; Kamman et al. 1988; Bartzokis et al., 2002). Complementary to assessing volumes of tissues on MRI, MR relaxometry describes quantitative changes in the MRI signal itself, using parameters that assess tissue integrity such as transverse relaxation rates (R_2; R_2 is defined as $1/T_2$, where T_2 is the transverse relaxation time). Work by Bartzokis and others has shown a decline in frontal lobe white matter (FLWM) R_2 that begins in the late 30's (peak at age 38) and markedly accelerates after about age 60. These data are consistent with the view that myelin breakdown may be a major factor in higher cognitive functions declining with age and may be accompanied by breakdown in white matter connectivity (Davatzikos et al., 2003). Histologic studies demonstrate that neuronal loss is minimal in normal aging (Terry et al., 1987), making Wallerian (axonal) degeneration an unlikely explanation for the white matter loss.

A precipitous decline in gray matter volume also occurs in both sexes after puberty (Fig. 3). The cellular basis of this change is more contentious, but it likely reflects reductions in dendritic arborization, dendritic length, synapse loss and other neuronal parameters. Earlier cross-sectional studies of normative brain maturation during childhood and adolescence have lead researchers to conclude that gray matter loss does occur as part of the ultimate sculpting of the brain into the fully functioning adult nervous system (Jernigan et al., 1991; Pfefferbaum et al., 1994; Reiss et al., 1996; Sowell et al., 1999, 2003). Gray matter loss has been observed consistently with

longitudinal MRI in late childhood and adolescence (Jernigan et al., 2001; Gogtay et al., 2004; Sowell et al., 2004). This loss is usually attributed to neuropil pruning seen histologically. The neuronal origin of these changes is supported, to some degree, by a general developmental decline in metabolites such as *N*-acetylaspartate, which are localized primarily in neurons, and can be observed *in vivo* using MR spectroscopy. It is also important to note here that the "loss" of gray matter observed with MRI during childhood and adolescence may also be associated with increases in myelination. Unmyelinated axonal and dendritic fibers presumably have an MRI signal value which is indistinguishable from that of gray matter. Thus, tissue in the peripheral neuropil that has a signal value like gray matter in the young child may continue to myelinate, resulting in a white matter signal value in the same individual as an adolescent. This hypothesis is further supported by recent evidence showing brain growth which spatially and temporally coincides with regional patterns of gray matter density *reduction* between childhood and young adulthood (Sowell et al., 2001b). If, in fact, gray matter "loss" was associated solely with regressive changes such as reductions in synaptic density, it is not likely that we would see continued brain growth in the same regions. Further studies using DTI may help disambiguate the potential cellular processes which contribute to the further sculpting of cortical structures during childhood.

To understand the anatomical sequence of these developmental brain changes, we now turn to a second method, cortical mapping. This method creates maps of gray matter changes in the cortex. By contrast with methods that measure regional volumes of brain tissues, cortical maps offer the ability to localize brain changes relative to the underlying gyral anatomy and visualize them in the form of statistical maps that reveal the topography of group differences.

4. Cortical Mapping

Mapping the Cortex. Figure 4 shows a general image analysis process, known as *cortical pattern matching*, that we developed for understanding how development and disease affect the cortex (Thompson et al., 2004). These methods have been used to reveal the profile of structural brain deficits childhood and adult-onset schizophrenia (Thompson et al., 2001; Cannon et al., 2002; Narr et al., 2004), attention-deficit/hyperactivity disorder (Sowell et al., 2003), fetal alcohol syndrome (Sowell et al., 2002), Tourette syndrome (Sowell et al., 2004), bipolar disorder (Gogtay et al., 2005), and Williams syndrome (Thompson et al., 2005). Below we describe some examples selected to illustrate the concepts.

The goal of cortical mapping is to create group average maps of cortical features of interest such as gray matter thickness, gray matter density, cortical shape, average sulcal patterning, and hemispheric asymmetries in these measures, all of which change during development. Next, statistics are defined that help localize group differences in these measures, such as brain structure differences between healthy children and those with neuropsychiatric disorders like schizophrenia or bipolar illness, or genetic disorders of brain development such as Williams syndrome. The resulting maps can reveal where in the brain differences are detected, how significant they are, and whether they are stable or progressive. Many variations on the basic mapping approach are possible. Any observed structural differences can also be correlated with measures such as medication or genotype, to investigate their origin and the potential effects of intervention. The same mapping techniques maps have also been used to assess functional differences in the cerebral and cerebellar cortex with functional MRI (see Rasser et al., 2004a,b; Zeineh et al., 2003 for examples).

The cortical mapping process is described in detail in Thompson et al., 2004, so we review it only briefly here. As shown in Fig. 4, brain MRI volumes pass through a number of preprocessing steps using several manual and automated procedures. First, we create an intracranial mask of the brain using a brain surface extraction algorithm tool (BSE) that is based on a combination of non-linear smoothing, edge detection and morphologic processing (Shattuck and Leahy, 2002). Any small errors in the masks are corrected manually to separate intracranial regions from surrounding extra-cranial tissue. Using these modified brain masks, all extra-cerebral tissues are removed from the image volumes. Brain masks and anatomical images are corrected for head alignment and individual differences in brain size by using an automatic 9-parameter linear registration (Woods et al., 1998) to transform

each brain volume into the target space of the ICBM-305 average brain created by the International Consortium for Brain Mapping (Mazziotta et al., 2001; Figure 4, step 1). After applying radiofrequency (RF) bias field corrections to eliminate intensity drifts due to magnetic field inhomogeneities in the scanner, each image volume is segmented into different tissue types by classifying voxels based on their signal intensity values (Shattuck et al., 2001; figure 4, step 2), followed by manually separating the left hemisphere from the right.

Next, *cortical pattern matching* methods (Thompson et al., 2004; Fig. 4, steps 3-7) are used to spatially relate homologous regions of cortex between subjects in order to permit the inter-individual comparison of cortical features, such as local cortical thickness, in equivalent surface locations. For that purpose, we create 3D cortical surface models for each hemisphere based on automatically generated mesh surfaces that are continuously deformed to fit a threshold intensity value that best differentiates extra-cortical cerebrospinal fluid from underlying cortical gray matter (MacDonald et al., 1998). The idea of this deformation process is to use a starting mesh which is deformed until its borders fit to a given intensity threshold of the respective image. As a result of the linear transformation procedure, the generated 3D cortical surface models correspond globally in size, orientation, and parameter space coordinates. Nevertheless, the same parameter space coordinates, within each cortical surface model, do not yet index the same anatomy across all subjects. Therefore, the cortical surface models from each individual are used to identify and manually outline the major cortical sulci on the brain surface. Detailed anatomic protocols for delineating cortical anatomy are available at http://www.loni.ucla.edu/~esowell/edevel/proto.html and have been previously validated, and their inter- and intra-rater reliability have been reported (Narr et al., 2001; Blanton et al., 2000; Sowell et al., 2002).

The manually derived sulcal landmarks are then used as anchors to drive the surrounding cortical surface anatomy of each individual into correspondence. During the surface-warping procedures, the algorithm computes a 3D vector deformation field that records the amount of x, y, and z coordinate shift (or deformation) associating the same cortical surface locations in each subject with reference to the average anatomical pattern of the entire study group (Thompson et al., 2004).

Tissue classified brain volumes are resampled to 0.33mm cubic voxels to improve the precision of subsequent thickness measurements. Cortical thickness – defined as the 3D distance (in mm) between inner gray matter/white matter border and the closest point on the outer surface (CSF/gray matter border) – is calculated using the Eikonal fire equation (Thompson et al., 2004) applied to voxels classified as gray matter. Cortical thickness is estimated voxel by voxel and projected as a local value (mm) onto the cortical surface. To increase detection sensitivity for group differences (i.e. signal to noise), a smoothing kernel is used to average thickness measures within a 15mm sphere at each cortical surface point (Figure 4, step 9).

Statistical Analysis. The mean values for cortical thickness (or any other cortical measure obtained at each cortical surface point) can be computed to provide maps of average cortical thickness across the entire cortical surface. Analysis of variance or multiple regression is then performed at each 3D cortical surface location to assess covariates of interest, such as possible effects of disease, gender and hemisphere and their potential interactions for cortical thickness. Uncorrected two-tailed probability values ($p<0.05$) from these tests are mapped directly onto the average cortical surface model of the entire sample providing detailed and spatially accurate maps of local thickness differences between groups. Regions where correlations exist between cortical thickness and symptoms or cognitive test scores can also be mapped (Figure 4, step 10), as can links with genotype, or even medication. Finally, permutation testing is employed to assign an overall significance value to the observed pattern of differences in the map (Thompson et al., 2004). For permutation testing, subjects are randomly assigned to groups, and a new statistical test is performed at each cortical surface point for each random assignment. The number of significant results from these randomizations is then compared to the number of significant results in the true assignment to produce a corrected overall significance value for the uncorrected statistical maps. The statistical validity of the findings can then be verified even in the presence of multiple comparisons and spatial correlations in the neuroimaging data.

Figure 5 shows some examples of cortical pattern matching applied to several developmental populations. We highlight examples of work on developmental disorders that are environmental in origin (e.g., fetal alcohol syndrome, which results from high maternal alcohol intake during embryonic development) as well as those that are primarily genetic in origin (e.g., Williams syndrome, which results from a chromosomal anomaly). The brain is most fragile during development, and anomalies of maturation can result from perturbations in genetic or environmental factors.

i. **Developing Brain Asymmetries.** The lateralization of brain function is of great interest in neuroscience as it provides vital information on the specialization of brain systems and the communication of information between brain hemispheres (see Toga and Thompson, 2003, for a review). Asymmetry is also of interest developmentally, as a number of disorders have been hypothesized to be associated with failures of the lateralization process, from dyslexia to schizophrenia (see Narr et al., 2004 for a study of schizophrenia using these methods). Cortical pattern matching provides a particularly attractive method to evaluate the magnitude and development of structural brain asymmetries. The pattern of asymmetries in sulcal patterning and gray matter thickness can be plotted spatially and related to chronological age or diagnosis. Figure 5(i)-(p) show some interesting maps of brain asymmetry in populations of different ages. In Thompson et al., 2001, we developed a general approach to map the mean profile of asymmetry in the gyral pattern, and assess its statistical significance, essentially by creating digital models of 3D curves representing sulci on the brain surface, and averaging their geometrical shapes across subjects. Regions can be distinguished that exhibit structural asymmetries that exceed the normal within-hemisphere variation in gyral patterning, and the anatomy of the right hemisphere can be seen to be shifted forwards by around 5-10 mm relative to the left. This asymmetry can be plotted on the mean sulcal pattern using a color code to emphasize regions where brain asymmetry is greatest. Sylvian fissures and superior temporal gyri exhibit the greatest asymmetries in the brain, with greatest values at their most posterior limits. Figure 5(i)-(k) show the mean pattern of asymmetry in groups of children, teenagers, and adults (data from Sowell et al., 2002). By computing mean geometric models of the cortical sulci, the models from one hemisphere can be 'mirrored' or reflected so that they can be compared with corresponding features in the opposite hemisphere. Then a 3D deformation map, or vector field, can be computed to express how much deformation would be required to force the left hemisphere mean sulcal pattern to match the right hemisphere sulcal pattern (see arrows in Fig. 5(l) and (m)). In elderly subjects, the gyral pattern asymmetry approaches 20 mm and is highly significant (Thompson et al., 2001; Fig. 5(n),(p)). The dynamic emergence of asymmetry in the developing human brain is yet one more feature for which normative statistical data has been established. This helps to delimit the range of normal variations in brain structure and distinguish them from variants outside of the normal range.

ii. **Fetal Alcohol Syndrome.** Intriguingly, very similar gray matter excesses in perisylvian zones were also observed in a recent study of fetal alcohol syndrome (FAS; Sowell et al., 2002). FAS subjects exhibited a 15% increase in gray matter density in the perisylvian and inferior parietal cortices bilaterally ($p < 0.001$, *L and R hems.*). Language systems may be especially vulnerable to alcohol neurotoxicity during cortical maturation, and excess cortical gray matter is most likely due to a failure of cortical formation during gyrogenesis, or a concomitant failure or delay in myelination, perhaps specifically in subcortical U-fibers (these two possibilities cannot be distinguished with conventional MRI).

iii. **Heritability and Brain Structure.** In the quest to understand what factors contribute to the trajectory of brain development, genetic and imaging methods can be combined to answer questions about the influence of genes and environment on brain structure. These methods are of two major types. The first of these methods uses twin or family designs to assess the proportion of genetic and environmental contribution to the observed variance in specific brain measures. By comparing the resemblance of relatives with different degrees of genetic relatedness, variance attributable to additive genetic, shared and unique environment can be established. The second approach also uses quantitative genetic modeling, but is based on modifying the concept of transmission disequilibrium to images. As a result, it is possible to

assess the effects of individual polymorphic markers on brain structure (Cannon et al., 2005). This provides enormous potential for relating developmental trajectories to information on normal and abnormal genetic variations.

The heritability of brain structure (i.e. proportion of observed variance explained by genetic variation in a population) can also be visualized in the form of a map. Figure 5 (panels q-t) shows several examples of maps identifying the degree to which genetic variations influence brain structure (Thompson et al., 2001, 2002). Essentially, MRI scans of identical and fraternal twins are compared and the degree of structural similarity is computed for a range of structural features - in this case cortical gray matter density - a measure related to cortical gray matter thickness (Thompson et al., 2004). Identical twins, who share all their genes, resembled each other more closely in brain structure than fraternal twins, who share only half their genes on average. This genetic control can be estimated quantitatively by examining intraclass correlations in brain measures between pairs of twins of each zygosity (i.e. identical or fraternal). The covariance of genetic affinity and structural affinity was highest for the volume of frontal gray matter in the brain, which, perhaps surprisingly, is almost entirely determined by genetic factors. In other words, the fact that each twin was exposed to different experiences throughout life made almost no difference to the quantity of gray matter. The quantity of frontal gray matter is moderately correlated with general cognitive ability as measured with standardized tests of intellectual function (or IQ), and IQ is also highly heritable (Thompson et al., 2001; Gray and Thompson, 2004; this link was replicated by Postuma et al., 2002). It is important to be aware of misinterpretations and misuses of heritability data, which have led to erroneous conclusions on the sources of individual and group differences in brain structure and cognition, and have led to a vitriolic debate (reviewed in Gray and Thompson, 2004). Because there can be strong gene by environment correlations, the proportion of genetic variance is not necessarily independent of, or at the expense of, environmental contributions to variance. The fact that a feature is heritable does not mean that it cannot be affected or manipulated by changes in the environment (see Gray and Thompson, 2004 for a discussion).

The almost complete genetic determination of gray matter volumes contrasts with the observed variation in sulcal and gyral patterns, which are less genetically constrained (Lohmann et al., 1999; see Thompson et al., 2001, 2003 for a review of neuroimaging studies of genetic influences on brain structure). Cerebellar volume exhibits almost zero heritability, despite the high heritability of cerebral volumes (Giedd et al., 2001). The search for heritable or genetically-mediated variations in brain structure is important as it can help identify features in images that are associated with imminent disease onset or liability for disorders such as schizophrenia (Cannon et al., 2002). Brain maps that link genes and structure can also better define the mechanisms and molecular pathways that lead to the organization of brain structure and deficits that imaging can identify. They also can be used to identify commonalities and unique signatures for specific developmental disorders, including systems where functional deficits may overlap in disorders with differing etiologies (Thompson et al., 2005, for an example on fetal alcohol and Williams syndrome).

iv. Williams Syndrome. Williams syndrome is an enigmatic developmental disorder associated with a deletion in the 7q11.23 chromosomal region (Korenberg et al., 2000). WS subjects have disrupted cortical development and mild to moderate mental retardation, but have relative proficiencies in language skills, social drive, and musical ability (Bellugi et al., 2000). Progress in understanding how this genetic anomaly impacts brain structure and behavior is impaired by the lack of detailed maps establishing the scope and anatomic extent of brain anomalies in WS. Figure 5 shows a series of maps that reveal that the cortical thickness in Williams syndrome is systematically increased in the perisylvian language area (data from Thompson et al., 2005). Based on MRI scans of 42 WS subjects and 40 matched controls, maps of individual cortical thickness were made (Figure 5(a)-(d)), and mean thickness maps compared between Williams syndrome patients (panel e) and controls (panel f). In WS, cortical thickness was significantly

increased (by 5-10%) in a discrete sector (panel g), encompassing perisylvian regions important for language function, specifically language comprehension. Against a backdrop of widespread brain tissue deficits, the perisylvian cortex was thicker than in controls, and this may partly account for the WS subjects' verbal strengths and unusually expressive language. Nonetheless the structural alterations in this study were not correlated with behavioral or cognitive measures so any links between structural and functional disturbances require further study to elucidate.

5. Time-Lapse Maps of Brain Change

An exciting extension of the maps described so far is the computation of *time-lapse maps* of brain structure. These show, using animation, spreading waves of cortical maturation in the developing brain, in spatial and temporal detail. Before introducing these dynamic maps, we review some of the major brain changes observable with MRI as healthy subjects age. Brain changes with aging can be viewed as a continuation of development, and the assessment of large imaging databases across the human lifespan can shed light on the waxing and waning of brain tissue volumes, with different trajectories for different regions of the brain.

Several studies have measured or mapped brain changes in children and adolescents scanned repeatedly during childhood and adolescence (Giedd et al., 1999; Thompson et al., 2000, 2001; Chung et al., 2001; Sowell et al., 1999, 2001, 2002, 2004; Gogtay et al., 2004). The dynamics of brain change across the adult human life span are highly nonlinear (Jernigan et al., 1991; Sowell et al., 2003). To help understand these changes, we recently developed a set of statistical mapping approaches to estimate nonlinear (quadratic) effects of aging on brain structure.

1. **Gray Matter Changes Over the Lifespan**. In a recent study (Sowell et al., 2003; Fig. 6(b) and (e)), we used MRI and cortical matching algorithms to map gray matter density (GMD) in 176 normal individuals aged 7 to 87 years. GMD declined nonlinearly with age, most rapidly between ages 7-60, over dorsal frontal and parietal association cortices, on both the lateral and interhemispheric surfaces. Age effects were inverted in the left posterior temporal region, where GMD gain continued up to age 30, and then rapidly declined. This was the first study to differentiate the trajectory of maturational and aging effects as they vary over the cortex. Visual, auditory and limbic cortices, which myelinate early, showed a more linear pattern of aging than the frontal and parietal neocortices, which continue myelination into adulthood. Posterior temporal cortices, primarily in the left hemisphere, which typically support language functions, have a more protracted course of maturation than any other cortical region, and myelination is the putative cause driving these changes.

2. **Time-Lapse Maps of Development**. Another developmental study (Gogtay et al., 2004) created a quantitative time-lapse map of human cortical development, reconstructed from serial brain MRI scans of 13 children aged 4-21. Dynamic video maps localizing brain changes were derived using high-dimensional elastic deformation mappings to match gyral anatomy across subjects and time. A quadratic statistical model, with random effects, was fitted to the profile of gray matter density against time, at each of the 65,536 cortical points (Fig. 6(c)). The resulting trajectory was animated to create a time-lapse movie [specific frames are shown in (d)]. This revealed a shifting pattern of gray matter loss, appearing first in dorsal parietal and primary sensorimotor regions near the interhemispheric margin, and spreading laterally and caudally into temporal cortices and anteriorly into dorsolateral prefrontal areas. This also supports findings of earlier studies (Giedd et al., 1999; Sowell et al., 1999), with a long-term longitudinal sample. The shifting profile of these changes is observed in a set of video sequences (see URL, http://www.loni.ucla.edu/~thompson/DEVEL/dynamic.html for several of these time-lapse movies).

3. **Brain-Behavior Relationships**. Changes in cortical thickness also relate to cognitive changes as children and adolescents mature. Sowell et al. (2004) found that cortical thinning in the left dorsal frontal and parietal lobes was correlated with improved performance on a test of general verbal intellectual functioning. To

establish this, cortical thickness in millimeters was computed from structural MR images of 45 children scanned twice (two years apart) between ages 5 and 11. Local brain growth progressed at a rate of approximately 0.4 to 1.5 mm per year, most prominently in frontal and occipital regions. Gray matter thinning coupled with cortical expansion was highly significant in right frontal and bilateral parieto-occipital regions. Forty-two of the studied children completed the Vocabulary subtest of the Wechsler Intelligence Scale for Children – Revised (Wechsler, 1991) at both scanning sessions. Negative correlations were observed primarily in the left hemisphere between the change scores and cortical thinning. Specifically, greater gray matter thinning was associated with improved performance on the Vocabulary subtest. Permutation analyses confirmed the significance of relationships between gray matter thinning and improved Vocabulary scores in the left lateral dorsal frontal ($p = 0.045$) and the left lateral parietal ($p = 0.030$) regions.

4. Childhood-Onset Schizophrenia. In developing time-lapse maps for clinical studies, there is a particular interest in modeling atrophic or developmental processes that speed up or slow down. Diseases may accelerate, or they may be slowed down by therapy. Among the most intriguing findings has been the observation of a progressively spreading wave of gray matter (GM) loss in subjects with childhood onset schizophrenia (COS; Thompson et al., 2001; Vidal et al., 2005; Figure 7). This medication-controlled study followed 12 subjects with COS every 2.5 years for 5 years, 12 matched healthy controls, and 10 medication-matched psychiatric controls, with serial MRI. As seen in Fig. 7 (left panels), healthy subjects lost gray matter at a subtle rate of 1-2% per year in parietal cortices. By contrast, the COS patients showed a more rapid progressive loss of GM in superior frontal and temporal cortices, reaching 3-4% per year in some local regions. The same pattern was replicated in both boys and girls, and agreed with early findings of progressive GM loss when the volumes of brain tissue in each of the lobes were assessed over time (Rapoport et al., 1999). Subtraction of the mean GM map in COS from the corresponding map for controls, at each time point, revealed a dynamic wave of gray matter loss in the COS patients (Fig. 7; *top right panels*). Early deficits in parietal brain regions that support language and associative thinking progressed anteriorly to temporal lobes, supplementary motor cortices and frontal eye fields. The deficits spread anatomically over a period of 5 years, consistent with the characteristic neuromotor, sensory and visual search impairments in the disease. In temporal cortices, including primary auditory regions, severe gray matter loss was absent at disease onset but became pervasive later in the disease. The spreading deficits are shown in a set of animation sequences (see URL, http://www.loni.ucla.edu/~thompson/MOVIES/SZ/sz.html). Several aspects of this study are noteworthy. First, as time-lapse maps of normal development are expanded to larger samples (Gogtay et al., 2004), it will be possible to assess whether the changes represent an acceleration of normally occurring brain changes (Gogtay et al., 2004), or a separate process entirely that begins in the adolescent years.

These time-lapse maps of COS may offer support or counterevidence when evaluating neurobiological models of the onset and progression of schizophrenia. The spreading patterns of deficits corroborate the idea that the normal process of dendritic and synaptic pruning may be abnormally accelerated or derailed in schizophrenia (Feinberg and Guazzelli, 1999). Nonetheless, the spreading deficits are quite different than those seen in neurodegenerative diseases, for example. Schizophrenia is not thought to be a neurodegenerative disorder due to the lack of gliosis in autopsy tissue from patients. Empirical studies also show that the degenerative sequence of dementia is anatomically selective, and quite different from that seen in schizophrenia. Figure 7 (*bottom right column*) shows the pattern of GM loss in a group of 12 patients with mild to moderate Alzheimer's disease, compared to 14 matched healthy elderly subjects (data from Thompson et al., 2003). Both cohorts were scanned longitudinally, and a time-lapse movie was created. Over a two-year period, the Alzheimer's patients exhibited a spreading wave of GM loss beginning in limbic and entorhinal cortices, spreading to frontal cortices, and sparing sensorimotor cortices. This is, in some respects, the opposite of the sequence of cortical maturation during development, in the sense that the primary sensory cortices mature first and degenerate last. Some have suggested that limbic regions have high neuronal plasticity throughout life and the resulting turnover of cellular metabolites makes them especially vulnerable to neurodegenerative disease (Mesulam et al., 2000).

The cellular basis of the progressive changes in COS is not clear. Progressive loss of frontal and temporal GM has been seen in first-episode adult-onset patients, and there is some evidence that it may be resisted, at least in adults, by atypical antipsychotics such as olanzapine (Keefe et al., 2004; Lieberman J., *pers. commun.*). Some histologic studies support the notion of decreased neuropil in schizophrenia, but autopsy material is relatively scarce in adolescent-onset populations and findings are inconsistent. This has led some to speculate that the cortical changes may be vascular or glial in origin, rather than purely neuronal (Weinberger and McClure, 2002). Intracortical contrast may also be affected by changes in myelination, and by changes in lipid metabolism during the use of atypical antipsychotics (Bartzokis et al., 2003). Second, the rate of GM loss may be unusually high in these severe, early onset cases, and may not be typical of schizophrenia in general. The loss rate would be expected to decelerate or plateau over a period of several years after the onset of psychosis.

With these caveats, time-lapse maps may still offer a biological marker of disease progression for medication trials. The gray matter differences have been found to correlate with fMRI measures in tasks that recruit the frontal lobes (Rasser et al., 2005). Frontal GM deficits have been observed in genetically at-risk relatives of patients (Cannon et al., 2002). Their magnitude may also provide a measure of imminent risk for disease. Progressive GM deficits have been seen in subjects in the prodromal phase of the illness, i.e., even before the first psychotic episode (Pantelis et al., 2003).

6. Mapping Brain Growth

A final question is whether these brain mapping techniques are applicable to mapping brain growth in individual children. In the examples presented so far, data from multiple subjects has been averaged together to create group average maps or time-lapse movies, and statistical maps have been computed to identify differences between groups of subjects. An interesting variation of these approaches is to compute maps of brain growth in an individual subject, using serial images to identify the region and rate of maximal growth in the brain.

Tensor Maps. One such approach for mapping brain growth, in an individual, is known as *tensor mapping* (Thompson et al., 2000), or tensor-based morphometry (Ashburner et al., 1998; Chung et al., 2001; Leow et al., 2005). This method essentially compares two scans of the same individual over time by elastically warping the earlier scan to match the later one. A high dimensional elastic deformation, or warping field, is calculated, typically with millions of degrees of freedom, which drives the baseline image to match its shape in a later scan (see Fig. 8). [These tensors have nothing to do with those that are mapped using diffusion imaging, which measure fiber orientation based on the directional properties and orientation of water diffusion in the brain]. The tensor that is mapped, in this context, is the gradient of the deformation field that warps the baseline to the later anatomy; mathematically it is equivalent to a 3x3 matrix attached to each point in the anatomy, which describes the principal directions of deformation at that point. The determinant of this matrix, called the Jacobian, is often used to summarize the transformation; this single number represents the local expansion factor (plotted in color in Fig. 8), and can be converted into a growth rate based on the time interval between scans. A notable feature of *tensors*, by contrast with displacement vectors, is that they distinguish intrinsic volumetric changes from bulk shifts in anatomy: unlike displacement vectors, tensors are invariant to translational shifts of a structure in stereotaxic space, but they are still sensitive to intrinsic volumetric changes. This distinction can help in studying developmental changes, as intrinsic changes in some structures may cause other structures to shift translationally. These two types of change usually will not be distinguished by voxel based methods, unless structures are perfectly aligned using high dimensional registration (Bookstein, 2001).

Corpus Callosum Growth. Fig. 8 shows typical results of a tensor mapping approach we developed to map growth of the corpus callosum (shown in Fig. 8, panel (a)) and basal ganglia in young children. We used it to detect an anterior-to-posterior wave of growth in the brains of children scanned repeatedly between the ages of 3 and 15 (Thompson et al., 2000). Parametric surface meshes were built to represent anatomical structures in a series of scans over time, and these were matched using a fully volumetric deformation. Dilation and contraction rates, and even the principal directions of growth, can be derived by examining the eigenvectors of the

deformation gradient tensor, or the local Jacobian matrix of the transform that maps the earlier anatomy onto the later one (Fig. 8). By analyzing the deformation fields, *tensor* maps can be created to reflect the magnitude and principal directions of tissue dilation or contraction. This mapping process is illustrated in Fig. 8. The validity of the approach can also be assessed by visualizing 'null maps' of brain change over short intervals. The increased spatial detail afforded by these mapping approaches makes them of particular interest for assessing fine-scale changes in anatomy during development.

Tensor-BasedMorphometry in Autistic Children Tensor maps may also be used to identify structural brain differences between two groups of subjects. Rather than warp the subject's anatomy at baseline onto a follow-up image from the same subject, all subjects' images are warped to match a common template. Highly flexible elastic or fluid transformations are used to deform the anatomy of each subject so it matches a template exactly. A measure of the dilation or contraction applied during this transformation (the Jacobian determinant) is an index of the local shape differences in anatomy across groups. Once registered across subjects, the resulting Jacobian determinant images may be analyzed using voxel based methods, an approach known as *tensor based morphometry* (TBM; Davatzikos et al., 1996; Chung et al., 2001; Ashburner et al., 1998). Recently, we used this method to identify white matter reductions in the corpus callosum of autistic children (Leow et al., 2005). Figure 8(d) and (e), respectively, show the average compression factor required to map normal children and autistic children to an average corpus callosum shape, and Figure 8(f) shows regions where these are different. White matter regions of the splenium were significantly reduced in autistic children. One benefit of this approach, as with the other mapping approaches, is that it does not require *a priori* specification of the regions in which differences are expected to occur. Regions can be searched for differences and multiple comparison corrections can be applied to make sure that any effects that are found are genuine.

7. Conclusion

In this chapter, we reviewed several of the major morphometric methods for mapping developmental changes in brain structure. As image analyses become increasingly automated, and as the scope and power of brain imaging studies expands to larger and more complex studies, substantial benefits will accrue. For developmental research in particular, key information is likely to come from the large-scale analysis of neuroimaging data, especially from children scanned longitudinally with MRI. Image analysis tools can now make time-lapse maps of developmental trajectories, as well as growth curves for individual structures. Future work will likely reveal factors that affect these developmental trajectories, both genetic and environmental. There is rapid progress in fusing genetic and neuroimaging methods for this purpose (Cannon et al., 2005).

This chapter has focused on mapping changes in brain structure with conventional MRI, but advances in other MRI techniques are now beginning to offer additional perspectives on the functional development of the brain. Functional MRI studies are now becoming more routine in young children, as are fiber mapping studies using diffusion tensor imaging, which previously required lengthy scanning protocols. Some of the more enigmatic changes in the cortex, described in this chapter, are likely to be ultimately understood by combining conventional imaging with spectroscopy and DTI, as each is sensitive to different aspects of cellular maturation.

As has been noted numerous times, the real power of these methods lies in identifying subtle developmental changes that would go unnoticed in individual images. No matter how large existing MRI databases become, specialized mathematics are still required to derive the most information from them. For example, mapping gene and medication effects on development is now within reach. Scan databases are only just now becoming large enough to stratify these cohorts by symptom profiles, therapeutic response, and currently identified risk factors. These studies are likely to help us better understand the links between neuroimaging markers and normal brain development, as well as the clinical course of developmental illnesses.

Figures

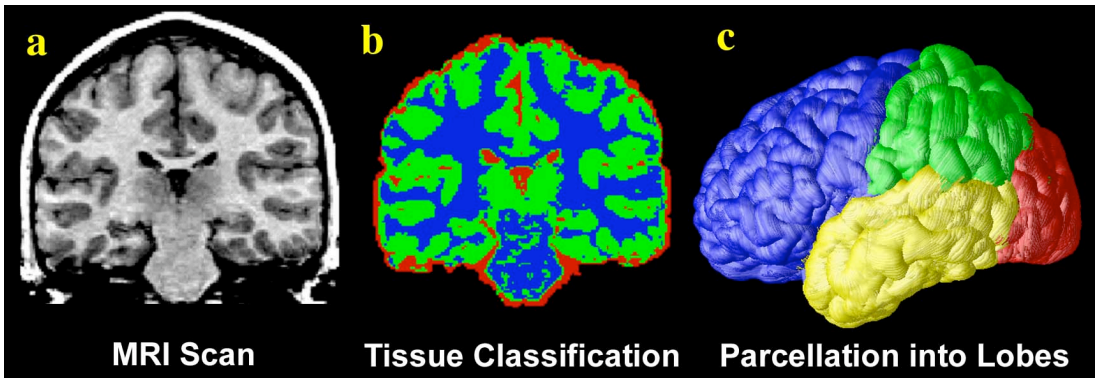

Figure 1. **Typical Processing Steps in an Analysis of MRI Brain Scans**. (a) shows a typical coronal section from a T1-weighted MRI scan of the brain. (b) is the result of applying a tissue classification approach to classify image voxels as gray matter (*green colors*), white matter (*blue colors*), or cerebrospinal fluid (CSF; *red colors*). Non-brain tissues such as scalp and meninges surrounding the brain have also been digitally edited from the image. (c) shows a parcellation of the brain into frontal lobe (*shown in blue*), parietal lobe (*green*), occipital lobe (*red*), and temporal lobe (*yellow*). This subdivision of anatomy is done with the aid of a cortical suface model on which sulcal landmarks separating the lobes can be reliably identified. Once partitioned in this way, the volumes of each tissue type in the major lobes can be computed and growth curves established for each major lobe.

Figures 2 and 3 are removed from the web version of this chapter, as they are under review for a peer-reviewed journal. Please check back later for an update of this chapter.

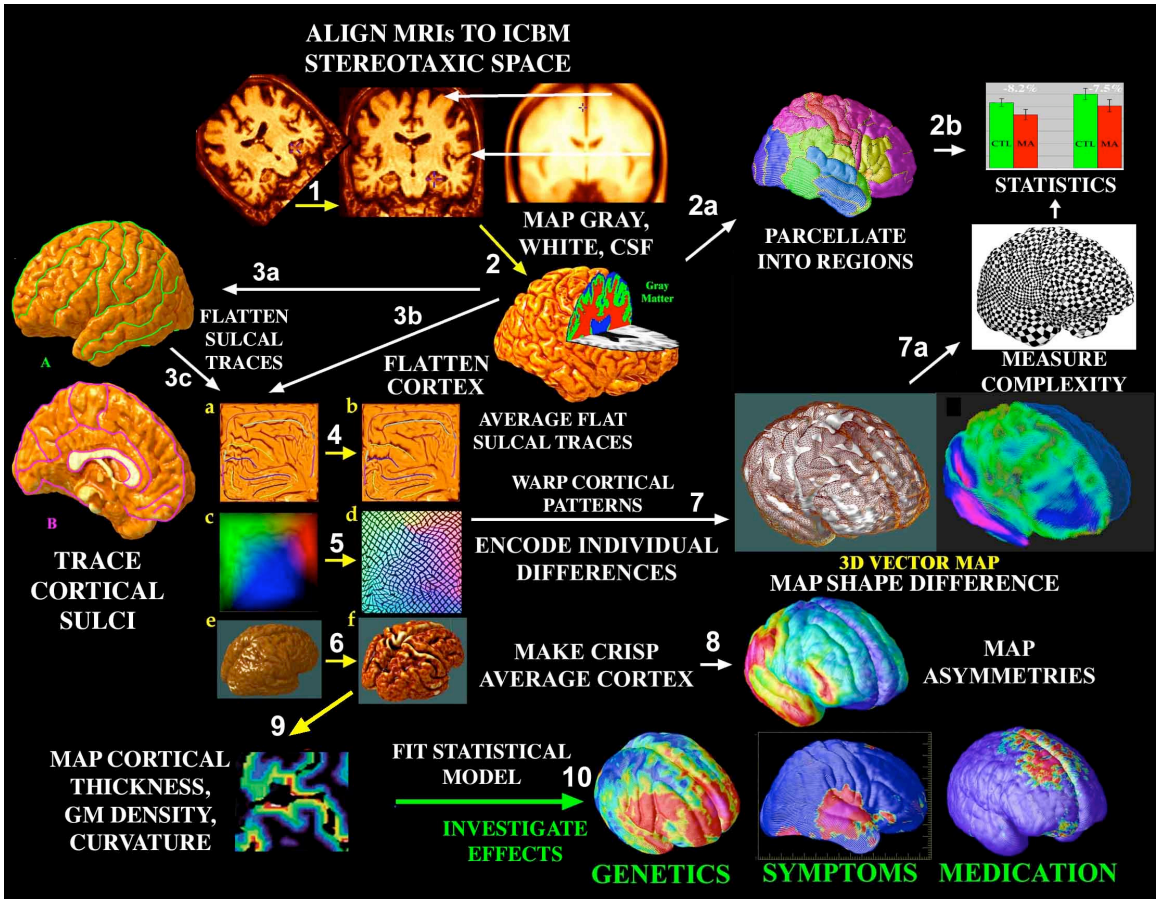

Figure 4. Image Analysis Steps for Detecting Developmental Changes and Group Differences in Cortical Anatomy. An image analysis pipeline is shown here. It can be used to create maps that reveal group differences and age-related changes in cortical thickness, gray matter density, gyral patterning, and asymmetries in these features. In general, 3D MRI scans from patients and controls are aligned (1) with an average brain template based on a population (here the ICBM template is used, developed by the International Consortium for Brain Mapping; Mazziotta et al., 2001). Tissue classification algorithms then generate maps of gray matter, white matter and CSF (2). In a simple analysis, these tissue maps can be parcellated into lobes (2a) and their volumes assessed with analysis of variance or other simple statistics (2b). Or, to compare cortical features from subjects whose anatomy differs, sulcal patterns can be traced onto individual cortical models, and used to guide the alignment of data from one subject to another. Individual sulcal curves and the surrounding cortical surfaces can then be flattened (3b, 3c) and aligned with a group average gyral pattern (4). If a color code indexing 3D cortical locations is flowed along with the same deformation field (5), a crisp group average model of the cortex can be made (6). Relative to this average, individual gyral pattern differences (7), measures of cortical complexity (7b), or cortical pattern asymmetry (8) can be computed. Once individual gyral patterns are aligned to the mean template, differences in gray matter density or thickness (9) can be mapped, after pooling data across subjects from homologous regions of cortex. Correlations can be identified between differences in gray matter density or cortical thickness and genetic risk factors (10). Maps may also be generated visualizing regions in which linkages are detected between structural deficits and clinical symptoms, cognitive scores, and medication effects, as well as changes in these parameters with age.

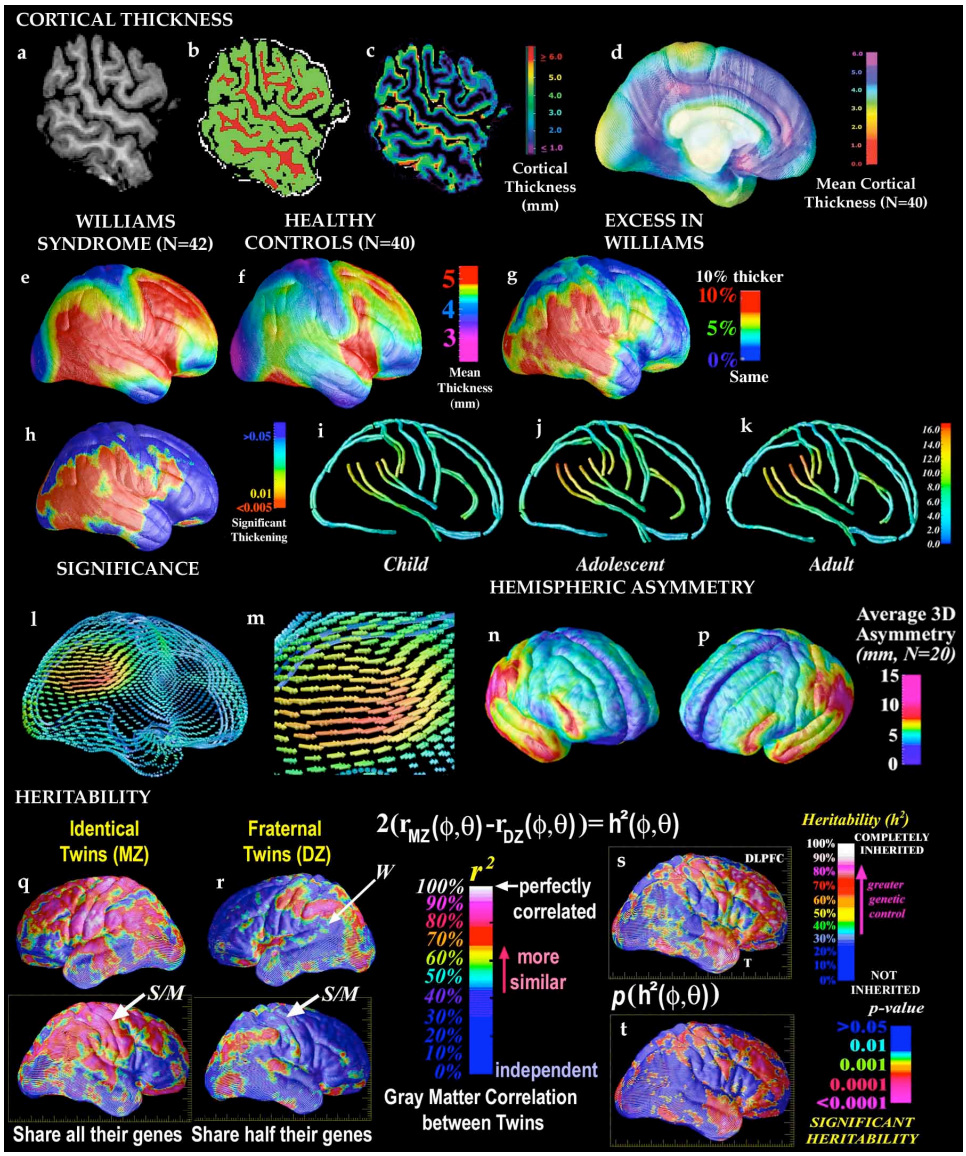

Figure 5. Statistical Maps of Cortical Structure. A variety of maps can be made that describe different aspects of cortical anatomy. These include maps of cortical thickness [(a)-(h)], gyral pattern asymmetry [(l)-(p)], and heritability of brain structure [(q)-(t)]. Explanations of these features are in the main text. Briefly, panels (a)-(d) show steps involved in measuring cortical thickness (for related work, see Jones et al., 2000; Annese et al., 2000; Fischl and Dale, 2000; Miller et al., 2000; Kruggel et al., 2001; Yezzi and Prince, 2001). In our approach, the MRI scan (a) is classified into gray matter, white matter, CSF, and a background class [respectively represented by green, red, black and white colors in (b)]. To quantify cortical gray matter thickness, we use the 3D distance measured from the cortical white-gray matter boundary in the tissue classified brain volumes to the cortical surface (gray-CSF boundary) in each subject (c). (d) shows the mean cortical thickness in a group of 40 healthy young adults, ranging from low values in primary sensorimotor and visual cortices (2-3 mm, *yellow colors*) to highest values on the medial wall in cingulate areas (up to 6 mm, *purple colors*). The regional variations in these maps agree with those found in the classical cortical thickness maps derived *post mortem* by von Economo (Sowell et al., 2004). (e) shows the profile of mean cortical thickness in Williams syndrome and healthy controls, and (g) shows the group difference expressed as a percentage of the control mean. Panels (i,j,k) show the increasing gyral pattern asymmetry in groups of children, adolescents, and adults (data from Sowell et al., 2002), computed from the 3D deformation fields (l,m) required to align the mean left hemisphere sulcal pattern to match a reflected version of the mean right hemisphere sulcal pattern. Asymmetry measures can also be extended to rest of the cortical surface (n,p) and expressed in millimeters. Panels (q) and (r) show intraclass correlations in gray matter density $g_{i,r}(\mathbf{x})$ for groups of identical and fraternal twins, after cortical pattern matching (giving maps $r_{MZ}(\phi,\theta)$ and $r_{DZ}(\phi,\theta)$). An estimate of gray matter heritability h^2 (panel (r)) can be defined as $2(r_{MZ}-r_{DZ})$, with standard error: $S.E.^2(h^2)=4[((1-r_{MZ}^2)^2/n_{MZ}) + ((1-r_{DZ}^2)^2/n_{DZ})]$. Regions in which significant genetic influences on brain structure are detected are shown in the significance map (panel (t)), $p[h^2(\phi,\theta)]$. Genetic influences on brain structure are pronounced in some frontal and temporal lobe regions, including the dorsolateral prefrontal cortex and temporal poles (denoted by *DLPFC* and *T* in (s)).

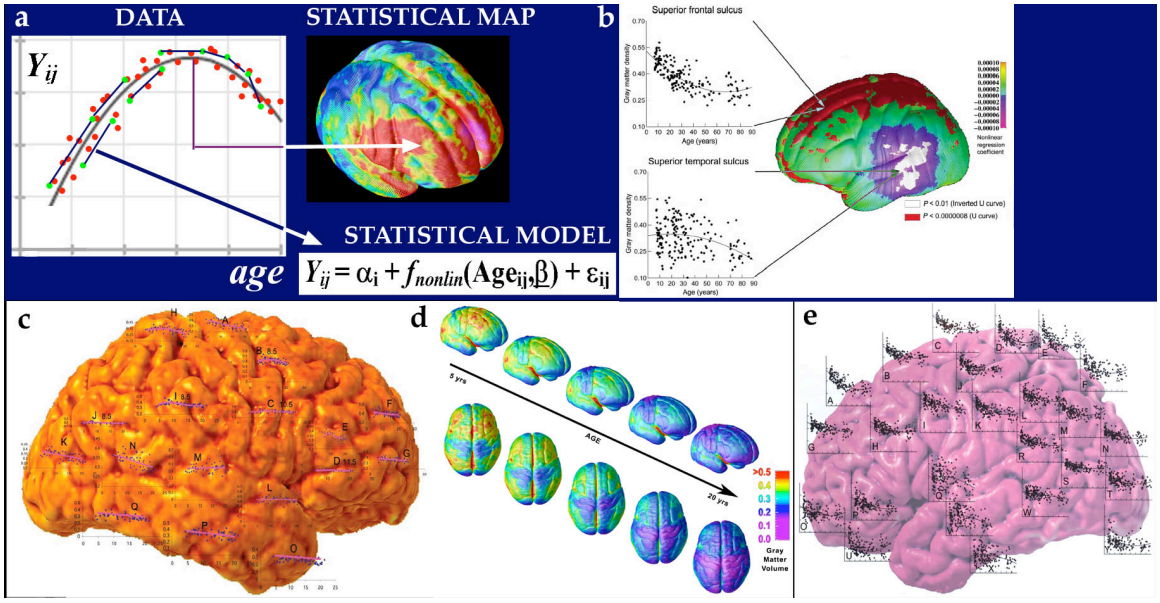

Figure 6. Mapping Brain Change over Time. The ability to resolve brain changes over time relies on fitting appropriate time-dependent statistical models to data collected from subjects cross sectionally, longitudinally, or both. Nonlinear or and/or mixed statistical models are fitted to brain maps collected at different ages to estimate the effects of brain aging or development on the cortex. As illustrated in (a), measures (Y_{ij}) are defined that can be obtained longitudinally (*green dots*) or once only (*red dots*) in a group of subjects at different ages. These measures might be gray matter density or cortical thickness, for example. Fitting of statistical models to these data (*Statistical Model, lower right*) produces estimates of significance values, or statistical parameters such as rates of change, or effects of drug treatment or risk genes. These parameters are then plotted onto the cortex using a color code. (b) and (e) show the trajectory of gray matter loss over the human lifespan, based on a cohort of 176 subjects aged between 7 and 87 (Sowell et al., 2003). (c) and (d) show the trajectory of cortical gray matter density in 13 children scanned longitudinally every 2 years for 8 years (Gogtay et al., 2004). [Data reproduced, with permission, from Gogtay et al., *Proceedings of the National Academy of Sciences*, 2004 [panels (c) and (d)], and from Sowell et al., *Nature Neuroscience*, 2003 [panels (b) and (e)]].

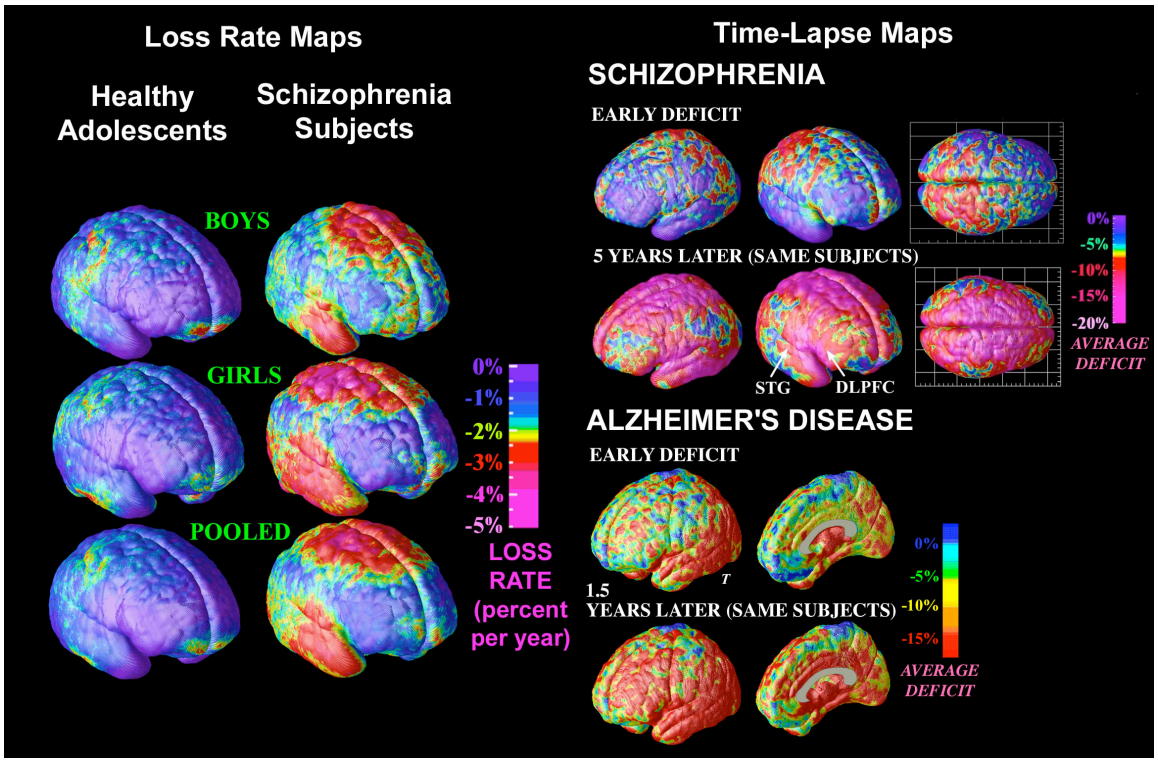

Figure 7. Rates of Brain Change in Childhood-Onset Schizophrenia and in Alzheimer's Disease. (left column): Average maps of gray matter loss rates are shown for healthy boys (*top row*), girls (*middle row*), and both genders pooled (*bottom row*), scanned longitudinally over 5 years. Also shown are maps of the considerably faster loss rates in age- and gender-matched subjects with childhood-onset schizophrenia (COS) also scanned at the same ages and intervals. The frontal cortex underwent a selective rapid loss of gray matter (up to 3-4% per year faster in patients than controls). Subtraction maps contrasting patients with controls revealed early deficits in parietal regions (*red colors*; *right column, top row*) that spread forwards into the rest of the cortex at follow-up [(*right column, second row*); superior temporal gyrus (STG) and the dorsolateral prefrontal cortex (DLPFC) are indicated with arrows]. These changes may be, in some respects, an exaggeration of changes that normally occur in adolescence (Rapoport et al., 1999; Thompson et al., 2001). By contrast, deficits occurring as Alzheimer's Disease (AD) progresses are show (*right column, bottom two rows*) by comparing average profiles of gray matter density between 12 AD patients (age: 68.4±1.9 yrs.) and 14 elderly matched controls (age: 71.4±0.9 yrs.; data from Thompson et al., 2003). Patients and controls are subtracted at their first scan (when mean Mini-Mental State Exam (MMSE) score=18 for the patients; *(right column, third row)*) and at their follow-up scan 1.5 years later (mean MMSE=13; *(right column, fourth row)*). In AD, gray matter loss sweeps forward in the brain from limbic to frontal cortices in concert with cognitive decline, but in the schizophrenia patients, the frontal cortices lose gray matter the fastest.

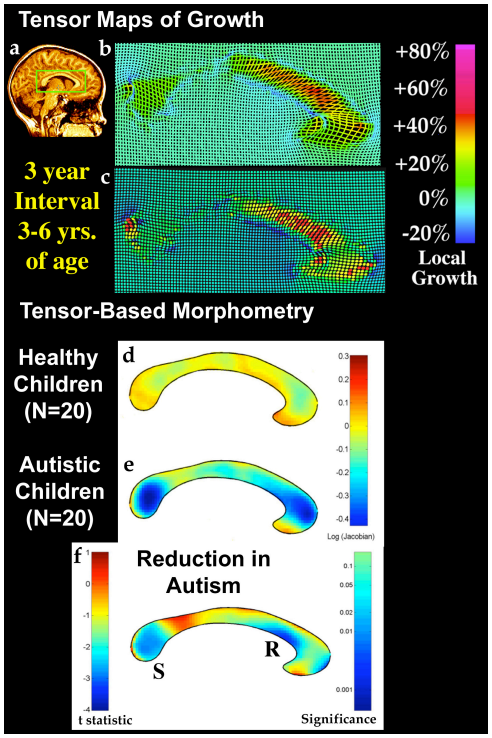

Figure 8. Tensor-Based Morphometry. (a) shows the corpus callosum of a healthy 3 year old girl (indicated by a *green box*) in a sagittal section from a 3D MRI scan. (b): Using a follow-up scan acquired 3 years later, an elastic deformation field is computed that digitally aligns, or warps, the anatomy of the earlier time-point to match its shape at the later time point. The amount of local stretching of the anatomy is coded in color in (b), indicating fastest growth rates (*red colors*) in the anterior corpus callosum. Mathematically, the growth rates are derived by evaluating the determinant (dilation factor) of the spatial gradient of the deformation vector field, which is a symmetric positive definite tensor field (c). In a related approach, maps can be compiled to represent the average expansion factor required to elastically deform an average corpus callosum shape onto each subject in a set of healthy children (d) and matched autistic children (e). When the logarithm of these expansion factors is taken (color coded in (d) and (e)), values below 0 denote contraction relative to the average. This logarithm transform is applied to reduce the skew in the Jacobian null distribution. Student's *t* tests (or other statistical models, such as the general linear model) may then be computed at each voxel in the expansion maps to localize group differences in structure. (f) shows in blue colors regions of the *splenium* (S) and *rostrum* (R) of the corpus callosum in which the cross sectional area is significantly reduced in the autistic children (data in (a)-(c) are adapted from Thompson et al., 2000, and data in (d)-(f) are adapted from from Leow et al., 2005).

References

Annese J, Pitiot A, Toga AW. 3D cortical thickness maps from histological volumes, NeuroImage 13(6)Part 2, S858, 2002.

Ashburner J, Hutton C, Frackowiak R, Johnsrude I, Price C, Friston K (1998). Identifying global anatomical differences: deformation-based morphometry. Hum Brain Mapping 1998;6(5-6):348-57.

Ballmeier M, Sowell ER, Thompson PM, Kumar A, Lavretsky H, Wellcome SE, DeLuca H, Toga AW (2003). *Mapping Brain Size and Cortical Surface Gray Matter Changes in Elderly Depression*, Biological Psychiatry 2004 Feb 15;55(4):382-9.

Bartzokis G, Beckson M, Lu PH, Nuechterlein KH, Edwards N,Mintz J. Age-related changes in frontal and temporal lobe volumes in men: A magnetic resonance imaging study. Arch Gen Psychiatry 2001;58:461-65.

Bartzokis G, Cummings J, Sultzer D, Henderson VW, Nuechterlein KH, Mintz J. White matter structural integrity in aging and Alzheimer's disease: A magnetic resonance imaging study. Arch Neurol 2003;60:393-398.

Bartzokis G, Sultzer D, Lu PH, Nuechterlein KH, Mintz J, Cummings JL (2004). Heterogeneous age-related breakdown of white matter structural integrity: implications for cortical "disconnection" in aging and Alzheimer's disease. Neurobiol Aging. 2004 Aug;25(7):843-51.

Bellugi U, Lichtenberger L, Jones W, Lai Z, St George M (2000). I. The neurocognitive profile of Williams Syndrome: a complex pattern of strengths and weaknesses. J Cogn Neurosci. 2000;12 Suppl 1:7-29. Review.

Blanton RE, Levitt JL, Thompson PM, Capetillo-Cunliffe LF, Sadoun T, Williams T, McCracken JT, Toga AW (2000). *Mapping Cortical Variability and Complexity Patterns in the Developing Human Brain*, Psychiatry Research 107:29-43, May 2000.

Bloch F (1946). Nuclear induction, Physical Review 70:460-473.

Bookstein F (2001). Voxel-Based Morphometry Should Not Be Used with Imperfectly Registered Images, Neuroimage, 2001.

Cannon TD, Hennah W, van Erp TGM, Thompson PM, Lonnqvist J, Huttunen M, Gasperoni T, Tuulio-Henriksson, Pirkola T, Toga AW, Kaprio J, Mazziotta JC, Peltonen L (2005). *DISC1/TRAX Haplotypes Associate with Schizophrenia, Reduced Prefrontal Gray Matter, and Impaired Short- and Long-Term Memory*, Archives of General Psychiatry [submitted].

Cannon TD, Thompson PM, van Erp T, Toga AW, Poutanen V-P, Huttunen M, Lönnqvist J, Standertskjöld-Nordenstam C-G, Narr KL, Khaledy M, Zoumalan CI, Dail R, Kaprio J. (2002) Cortex mapping reveals regionally specific patterns of genetic and disease-specific gray-matter deficits in twins discordant for schizophrenia. Proc Natl Acad Sci U S A 99:3228-33.

Cannon TD, Thompson PM, van Erp TGM, Huttunen M, Lonnqvist J, Kaprio J, Toga AW (2005). *Mapping Heritability and Molecular Genetic Associations with Cortical Features Using Probabilistic Brain Atlases: Methods and Initial Applications to Schizophrenia*, Neuroinformatics [submitted, Dec. 2004].

Chung, M.K., Worsley, K.J., Paus, T., Cherif, C., Giedd, J.N., Rapoport, J.L, Evans, A.C. (2001) A Unified Statistical Approach to Deformation-Based Morphometry, NeuroImage 14:595-606.

Collins DL, Holmes CJ, Peters TM, Evans AC (1995). *Automatic 3D Model-Based Neuroanatomical Segmentation*, Human Brain Mapping 3:190-208.

Courchesne E, Chisum HJ, Townsend J, Cowles A, Covington J, Egaas B, Harwood M, Hinds S, Press GA (2000) Normal brain development and aging: quantitative analysis at in vivo MR imaging in healthy volunteers. Radiology 216:672-682.

Csernansky JG, Joshi S, Wang L, et al. Hippocampal morphometry in schizophrenia by high dimensional brain mapping. Proc Natl Acad Sci U S A 1998;95(19):11406-11411.

Davatzikos C, Resnick SM. Degenerative age changes in white matter connectivity visualized in vivo using magnetic resonance imaging. Cerebral Cortex. In press 2003

Davatzikos C, Vaillant M, Resnick SM, Prince JL, Letovsky S, Bryan RN (1996). A Computerized Approach for Morphological Analysis of the Corpus Callosum, J. Comp. Assisted Tomography, 20(1):88-97.

Davidian, M., Giltinan, DM, Nonlinear Models for Repeated Measurement Data, Chapman & Hall, First Edition, 1995.

Elster AD (1994). Questions and Answers in MRI (Mosby).

Englund E, Brun A, Persson B (1987): Correlations between histopathologic white matter changes and proton MR relaxation times in dementia. *Alzheimer Dis Assoc Discord* 1:56-70.

Feinberg I, Guazzelli M (1999). Schizophrenia--a disorder of the corollary discharge systems that integrate the motor systems of thought with the sensory systems of consciousness, Br J Psychiatry. 1999 Mar;174:196-204.

Fischl B, Dale AM (2000). Measuring the thickness of the human cerebral cortex from magnetic resonance images. Proc Natl Acad Sci U S A. 2000 Sep 26;97(20):11050-5.

Giedd JN, Greenstein D, Blumenthal J, Wallace G, Gogtay N, Lenroot RH (2005). Sexual Dimorphism of Human Brain Developmental Trajectories During Childhood and Adolescence, [submitted].

Giedd JN, Molloy E, Vaituzis AC, Blumenthal J, Clasen L, Liu H, Castellanos FX, Thompson PM (2001). Heritability of cerebral cortex morphometry during childhood and adolescence. Proc. Amer. Coll. Neuropsychopharmacology (ACNP). Waikoloa Village, Hawaii, December 2001.

Giedd JN, Blumenthal J, Jeffries NO, Castellanos FX, Liu H, Zijdenbos A, Paus T, Evans AC, Rapoport JL.. Brain development during childhood and adolescence: a longitudinal MRI study. *Nat Neurosci* 1999 Oct;2(10):861-3 (1999b).

Giedd JN, Jeffries NO, Blumenthal J, Castellanos FX, Vaituzis AC, Fernandez T, Hamburger SD, Liu H, Nelson J, Bedwell J, Tran L, Lenane M, Nicolson R, Rapoport JL. (1999). Childhood-onset schizophrenia: progressive brain changes during adolescence. *Biol. Psychiatry* 46(7):892-8 (1999a).

Gogtay N, Giedd JN, Lusk L, Hayashi KM, Greenstein D, Vaitiuzis C, Nugent TF, Herman DH, Classen L, Toga AW, Rapoport JL, Thompson PM (2004). *Dynamic Mapping of Human Cortical Development During Childhood and Adolescence*, Proceedings of the National Academy of Sciences, 101(21):8174-8179, May 25 2004.

Gogtay N, Herman DH, Ordonez A, Hayashi KM, Greenstein D, Vaituzis C, Clasen L, Sporn A, Giedd JN, Nugent TF, Toga AW, Leibenluft E, Thompson PM, Rapoport JL (2005). Cortical Development in Early Onset Bipolar Illness Before and After Illness Onset [submitted].

Gray JR, Thompson PM (2004). *Neurobiology of Intelligence: Science and Ethics*, Nature Reviews Neuroscience, 2004 Jun;5(6):471-82.

Jernigan TL, Archibald SL, Fennema-Notestine C, Gamst AC, Stout JC, Bonner J, Hesselink JR (2001). Effects of age on tissues and regions of the cerebrum and cerebellum. Neurobiol Aging. 2001 Jul-Aug;22(4):581-94.

Jernigan TL, Trauner DA, Hesselink JR, Tallal PA (1991) Maturation of human cerebrum observed in vivo during adolescence. Brain 114:2037-2049.

Jones SE, Buchbinder BR, Aharon I. Three-dimensional mapping of cortical thickness using Laplace's equation. Hum Brain Mapp 2000;11(1):12-32.

Kamman RL, Go KG, Brouwer W, Berendsen HJ (1988). Nuclear magnetic resonance relaxation in experimental brain edema: effects of water concentration, protein concentration, and temperature. Magn Reson Med. 1988 Mar;6(3):265-74.

Keefe RS, Seidman LJ, Christensen BK, Hamer RM, Sharma T, Sitskoorn MM, Lewine RR, Yurgelun-Todd DA, Gur RC, Tohen M, Tollefson GD, Sanger TM, Lieberman JA (2004). Comparative effect of atypical and conventional antipsychotic drugs on neurocognition in first-episode psychosis: a randomized, double-blind trial of olanzapine versus low doses of haloperidol. Am J Psychiatry. 2004 Jun;161(6):985-95.

Kennedy DN, Lange N, Makris N, Bates J, Meyer J, Caviness VS Jr. (1998). Gyri of the human neocortex: an MRI-based analysis of volume and variance. Cerebral Cortex, 1998 Jun, 8(4):372-84.

Kimura D (1999). Sex and Cognition, Cambridge, MA: MIT Press.

Kruggel F, Bruckner MK, Arendt T, Wiggins CJ, von Cramon DY. Analyzing the neocortical fine structure. In: Proc Info Process in Med Imaging; 2001: Springer Press, 2001: 239-245.

Lange N, Giedd JN, Castellanos FX, Vaituzis AC, Rapoport JL (1997). Variability of human brain structure size: ages 4-20 years. Psychiatry Res. 1997 Mar 14;74(1):1-12.

Lauterbur PC (1973). Image formation by induced local interactions: Examples employing nuclear magnetic resonance, Nature 242: 190-191, 1973.

Leow A, Yu CL, Lee SJ, Huang SC, Nicolson R, Hayashi KM, Protas H, Toga AW, Thompson PM (2005). *Brain Structural Mapping using a Novel Hybrid Implicit/Explicit Framework based on the Level-Set Method*, NeuroImage, February 2005.

Lin JJ, Salamon N, Lee AD, Dutton RA, Geaga JA, Hayashi KM, London ED, Toga AW, Engel J, Thompson PM (2004). *Mapping of Neocortical Gray Matter Loss in Patients with Mesial Temporal Lobe Epilepsy with Hippocampal Sclerosis*, Proc. 34th Annual Conference of the Society for Neuroscience, San Diego, CA, Oct. 23-27 2004.

Lohmann G, von Cramon DY, Steinmetz H (1999). Sulcal variability of twins. Cereb Cortex. 1999 Oct-Nov;9(7):754-63.

Luders E, Narr KL, Thompson PM, Rex DE, Jancke L, Toga AW (2004). *Gender Differences in Cortical Complexity*, Nature Neuroscience, 7(8):799-800, Aug. 2004.

Luders E, Narr KL, Thompson PM, Rex DE, Woods RP, DeLuca H, Jancke L, Toga AW (2005). Gender Effects on Cortical Thickness and the Influence of Scaling, [submitted].

Luders E, Narr KL, Woods RP, Rex DE, Thompson PM, Jancke L, Steinmetz H, Toga AW (2005). *Mapping Cortical Gray Matter in the Young Adult Brain: Effects of Gender*, [submitted].

Luders E, Thompson PM, Narr KL, Toga AW, Jancke L, Gaser C (2005). *A Surface Shape-based Approach to Local Cortical Complexity*, [submitted, Dec. 2004].

MacDonald D (1998). A Method for Identifying Geometrically Simple Surfaces from Three Dimensional Images, PhD Thesis, McGill Univ., Canada.

Mazziotta JC, Toga AW, Evans AC, Fox PT, Lancaster J, Zilles K, Woods RP, Paus T, Simpson G, Pike B, Holmes CJ, Collins DL, Thompson PM, MacDonald D, Schormann T, Amunts K, Palomero-Gallagher N, Parsons L, Narr KL, Kabani N, Le Goualher G, Boomsma D, Cannon T, Kawashima R, Mazoyer B (2001). *A Probabilistic Atlas and Reference System for the Human Brain [Invited Paper],* Journal of the Royal Society 356(1412):1293-1322, 29th August 2001.

Mesulam MM (2000). A plasticity-based theory of the pathogenesis of Alzheimer's disease. Ann N Y Acad Sci 2000;924:42-52.

Miller MI, Massie AB, Ratnanather JT, Botteron KN, Csernansky JG. Bayesian construction of geometrically based cortical thickness metrics. Neuroimage 2000;12(6):676-687.

Narr KL, Bilder RM, Toga AW, Woods RP, Rex DE, Szeszko PR, Robinson D, Sevy S, Gunduz-Bruce H, Wang YP, DeLuca H, Thompson PM (2004). *Mapping Cortical Thickness and Gray Matter Concentration in First Episode Schizophrenia*, Cerebral Cortex, 2004 Sep 15; [Epub ahead of print].

Narr KL, Cannon TD, Woods RP, Thompson PM, Kim S, Asunction D, van Erp TG, Poutanen VP, Huttunen M, Lonnqvist J, Standerksjold-Nordenstam CG, Kaprio J, Mazziotta JC, Toga AW (2002). Genetic contributions to altered callosal morphology in schizophrenia. Journal of Neuroscience, May 1, 22(9):3720-9.

Narr KL, Thompson PM, Sharma T, Moussai J, Blanton R, Anvar B, Edris A, Krupp R, Rayman J, Khaledy M, Toga AW (2001). Three-dimensional mapping of temporo-limbic regions and the lateral ventricles in schizophrenia: gender effects. Biol Psychiatry. 2001 Jul 15;50(2):84-97.

Narr KL, Thompson PM, Sharma T, Moussai J, Cannestra AF, Toga AW (2000). *Mapping Corpus Callosum Morphology in Schizophrenia*, Cerebral Cortex, 10(1):40-49, January 2000.

Narr KL, Thompson PM, Sharma T, Moussai J, Zoumalan CI, Rayman J, Toga AW (2001). *3D Mapping of Gyral Shape and Cortical Surface Asymmetries in Schizophrenia: Gender Effects*, Am J Psychiatry 2001 Feb 1;158(2):244-255.

Narr KL, Toga AW, Szeszko P, Thompson PM, Woods RP, Robinson D, Sevy S, Wang YP, Schrock K, Bilder RM (2005). *Cortical Thinning in Cingulate and Occipital Cortices in First Episode Schizophrenia*, [submitted, Nov. 2004].

Nielsen K, Peters A (2000): The effects of aging on the frequency of nerve fibers in rhesus monkey striate cortex. *Neurobiol Aging* 21:621-628.

Pantelis C, Velakoulis D, McGorry PD, Wood SJ, Suckling J, Phillips LJ, Yung AR, Bullmore ET, Brewer W, Soulsby B, Desmond P, McGuire PK (2003). Neuroanatomical abnormalities before and after onset of psychosis: a cross-sectional and longitudinal MRI comparison. Lancet. 2003 Jan 25;361(9354):281-8.

Peters A, Morrison JH, Rosene DL, Hyman BT (1998): Feature article: are neurons lost from the primate cerebral cortex during normal aging? *Cereb Cortex* 8:295-300.

Pfefferbaum A, Mathalon DH, Sullivan EV, Rawles JM, Zipursky RB, Lim KO (1994) A quantitative magnetic resonance imaging study of changes in brain morphology from infancy to late adulthood. Arch Neurol 51:874-887.

Posthuma D, De Geus EJ, Baare WF, Hulshoff Pol HE, Kahn RS, Boomsma DI (2002). The association between brain volume and intelligence is of genetic origin. Nat Neurosci. 2002 Feb;5(2):83-4.

Rapoport JL, Giedd J, Kumra S, Jacobsen L, Smith A, Lee P, Nelson J, Hamburger S (1997). Childhood-onset schizophrenia. Progressive ventricular change during adolescence [see comments]. *Arch Gen Psychiatry* 54:897-903 (1997).

Rapoport JL, Giedd JN, Blumenthal J, Hamburger S, Jeffries N, Fernandez T, Nicolson R, Bedwell J, Lenane M, Zijdenbos A, Paus T, Evans A (1999). Progressive cortical change during adolescence in childhood-onset schizophrenia. A longitudinal magnetic resonance imaging study. Arch Gen Psychiatry. 1999 Jul;56(7):649-54.

Rasser PE, Johnston PJ, Lagopoulos J, Ward PB, Schall U, Thienel R, Bender S, Toga AW, Thompson PM (2004). *Analysis of fMRI BOLD activation during the Tower of London Task using Gyral Pattern and Intensity Averaging Models of Cerebral Cortex*, NeuroImage [2nd revision submitted].

Reiss AL, Abrams MT, Singer HS, Ross JL, Denckla MB (1996) Brain development, gender and IQ in children. A volumetric imaging study. Brain 119:1763-1774.

Shattuck DW, Sandor-Leahy SR, Schaper KA, Rottenberg DA, Leahy RM (2001). Magnetic resonance image tissue classification using a partial volume model. Neuroimage. 2001 May;13(5):856-76.

Sowell ER, Levitt J, Thompson PM, Holmes CJ, Blanton RE, Kornsand DS, Caplan R, McCracken J, Asarnow R, Toga AW (1999). *Brain Abnormalities in Early-Onset Schizophrenia Spectrum Disorder Observed with Statistical Parametric Mapping of Structural Magnetic Resonance Images*, American Journal of Psychiatry 157(9):1475-84, Sept. 2000.

Sowell ER, Peterson BS, Thompson PM, Welcome SE, Henkenius AL, Toga AW (2003). *Mapping Cortical Change Across the Human Lifespan*, Nature Neuroscience, 6(3):309-15, March 2003.

Sowell ER, Thompson PM, Holmes CJ, Jernigan TL, Toga AW (1999) In vivo evidence for post-adolescent brain maturation in frontal and striatal regions. Nature Neuroscience 2:859-861.

Sowell ER, Thompson PM, Leonard CM, Welcome SE, Kan E, Toga AW (2004) Longitudinal Mapping of Cortical Thickness and Brain Growth in Normal Children. Journal of Neuroscience 24(38):8223-31.

Sowell ER, Thompson PM, Peterson BS, Mattson SN, Welcome SE, Henkenius AL, Riley EP, Jernigan TL, Toga AW (2002). *Mapping Cortical Gray Matter Asymmetry Patterns in Adolescents with Heavy Prenatal Alcohol Exposure*, Neuroimage, 17(4):1807-19, Dec. 2002.

Sowell ER, Thompson PM, Rex DE, Kornsand DS, Jernigan TL, Toga AW (2002). *Mapping Sulcal Pattern Asymmetry and Local Cortical Surface Gray*

Matter Distribution In Vivo: Maturation in Perisylvian Cortices, Cerebral Cortex 12(1):17-26, Jan. 2002.

Sowell ER, Mattson SN, Thompson PM, Jernigan TL, Riley EP, Toga AW (2001a) Mapping Callosal Morphology and Cognitive Correlates: Effects of Heavy Prenatal Alcohol Exposure. Neurology 57:235-244.

Sowell ER, Thompson PM, Tessner KD, Toga AW (2001b) Mapping continued brain growth and gray matter density reduction in dorsal frontal cortex: Inverse relationships during postadolescent brain maturation. J Neurosci 21:8819-8829.

Sowell ER, Thompson PM, Toga AW (2004). *Mapping Changes in the Human Cortex Throughout the Span of Life* [Invited Review], The Neuroscientist, 10(4):372-92, August 2004.

Sowell ER, Thompson PM, Welcome SE, Henkenius AL, Toga AW, Peterson BS (2003). *Cortical Abnormalities in Children and Adolescents with Attention-Deficit Hyperactivity Disorder*, The Lancet, 22:362(9397):1699-1707, December 2003.

Sowell ER, Thompson PM, Yoshii J, Kan E, Toga AW, Peterson BS (2004). Gray Matter Thickness Abnormalities Mapped in Children with Tourette Syndrome, Proc. 34th Annual Conference of the Society for Neuroscience, San Diego, CA, Oct. 23-27 2004.

Terry RD, DeTeresa R, Hansen LA (1987): Neocortical cell counts in normal human adult aging. *Ann Neurol* 21:530-539.

Thompson PM, Cannon TD, Narr KL, van Erp T, Khaledy M, Poutanen V-P, Huttunen M, Lönnqvist J, Standertskjöld-Nordenstam C-G, Kaprio J, Dail R, Zoumalan CI, Toga AW (2001). *Genetic Influences on Brain Structure,* Nature Neuroscience 4(12):1253-8, Dec. 2001.

Thompson PM, Cannon TD, Toga AW (2002). *Mapping Genetic Influences on Human Brain Structure* [Review Paper], Annals of Medicine, 2002;34(7-8):523-36.

Thompson PM, Giedd JN, Woods RP, MacDonald D, Evans AC, Toga AW (2000). *Growth Patterns in the Developing Brain Detected By Using Continuum-Mechanical Tensor Maps*, Nature, 404:(6774) 190-193, March 9, 2000.

Thompson PM, Hayashi KM, de Zubicaray G, Janke AL, Rose SE, Semple J, Herman D, Hong MS, Dittmer S, Doddrell DM, Toga AW (2003). *Dynamics of Gray Matter Loss in Alzheimer's Disease,* Journal of Neuroscience, 23(3):994-1005, Feb. 1 2003.

Thompson PM, Hayashi KM, de Zubicaray G, Janke AL, Rose SE, Semple J, Hong MS, Herman D, Gravano D, Doddrell DM, Toga AW (2004). *Mapping Hippocampal and Ventricular Change in Alzheimer's Disease*, NeuroImage, 22(4):1754-66, Aug. 2004; published online, June 1, 2004.

Thompson PM, Hayashi KM, Simon S, Geaga J, Hong MS, Sui Y, Lee JY, Toga AW, Ling WL, London ED (2004). *Structural Abnormalities in the Brains of Human Subjects who use Methamphetamine,* Journal of Neuroscience*,* 24(26):6028-6036, June 30 2004.

Thompson PM, Hayashi KM, Sowell ER, Gogtay N, Giedd JN, Rapoport JL, de Zubicaray GI, Janke AL, Rose SE, Semple J, Doddrell DM, Wang YL, van Erp TGM, Cannon TD, Toga AW (2004). *Mapping Cortical Change in Alzheimer's Disease, Brain Development, and Schizophrenia*, Special Issue on *Mathematics in Brain Imaging* (Thompson PM, Miller MI, Ratnanather JT, Poldrack R, Nichols TE, eds.), NeuroImage, 23 Suppl 1:S2-18, September 2004.

Thompson PM, Lee AD, Dutton RA, Geaga JA, Hayashi KM, Eckert MA, Bellugi U, Galaburda AM, Korenberg JR, Mills DL, Toga AW, Reiss AL (2005). Cortical Complexity and Thickness are Increased in Williams Syndrome, Journal of Neuroscience [revised, Dec. 2004].

Thompson PM, Mega MS, Vidal C, Rapoport JL, Toga AW (2001). Detecting Disease-Specific Patterns of Brain Structure using Cortical Pattern Matching and a Population-Based Probabilistic Brain Atlas, IEEE Conference on Information Processing in Medical Imaging (IPMI), UC Davis, 2001, in: Lecture Notes in Computer Science (LNCS) 2082:488-501, M Insana, R Leahy [eds.], Springer-Verlag.

Thompson PM, Schwartz C, Lin RT, Khan AA, Toga AW (1996). 3D Statistical Analysis of Sulcal Variability in the Human Brain, Journal of Neuroscience, Jul. 1996, 16(13):4261-4274.

Thompson PM, Toga AW (2002). *A Framework for Computational Anatomy* [Invited Paper], Computing and Visualization in Science, 5:1-12.

Thompson PM, Vidal CN, Giedd JN, Gochman P, Blumenthal J, Nicolson R, Toga AW, Rapoport JL (2001). *Mapping Adolescent Brain Change Reveals Dynamic Wave of Accelerated Gray Matter Loss in Very Early-Onset Schizophrenia*, Proceedings of the National Academy of Sciences of the USA, 98(20):11650-11655, September 25, 2001.

Thompson PM, Woods RP, Mega MS, Toga AW (2000). Mathematical/Computational Challenges in Creating Population-Based Brain Atlases, Human Brain Mapping 9(2):81-92, Feb. 2000.

Thompson, P.M., Narr, K.L., Blanton, R.E., Toga, A.W. (2003). *Mapping Structural Alterations of the Corpus Callosum during Brain Development and Degeneration*, Book Chapter in: Marco Iacoboni, Eran Zaidel [eds.], *The Parallel Brain*, MIT Press, Cambridge.

Toga AW, Thompson PM (2003). *Mapping Brain Asymmetry*, Nature Reviews Neuroscience, 4(1):37-48, January 2003.

Verbeke G, Molenberghs G (2000). Linear mixed models for longitudinal data. - New York: Springer, 2000.

Vidal CN, Thompson PM, Hayashi KM, Geaga JA, Sui Y, McLemore LE, Alaghband Y, Giedd JN, Gochman P, Blumenthal J, Gogtay N, Nicolson R, Toga AW, Rapoport JL (2005). *Dynamically Spreading Frontal and Cingulate Deficits Mapped in Adolescents with Schizophrenia*, [submitted, Archives of General Psychiatry, July 2004].

Von Economo CV (1929) The Cytoarchitectonics of the Human Cerebral Cortex. London: Oxford Medical Publications.

Wechsler D (1991) Manual for the Wechsler Intelligence Scale for Children - Third Edition. San Antonio, TX: The Psychological Corporation.

Weinberger DR, McClure RK (2002). Neurotoxicity, neuroplasticity, and magnetic resonance imaging morphometry: what is happening in the schizophrenic brain? Arch Gen Psychiatry. 2002 Jun;59(6):553-8. Review.

Woods RP, Mazziotta JC, Cherry SR (1993) MRI-PET registration with automated algorithm. Journal of Computer Assisted Tomography 17:536-546.

Yezzi A, Prince J. A PDE approach for measuring tissue thickness. In: CVPR; 2001; Kauai, 2001.

Zeineh MM, Engel SA, Thompson PM, Bookheimer S (2003). *Dynamics of the Hippocampus During Encoding and Retrieval of Face-Name Pairs*, Science, 299(5606):577-580, January 24 2003.